Malaysian Journal of Chemistry, 2023, Vol. 25(2), 153-163
(*Special Theme: Women in Chemistry*)

Environmentally Friendly Synthesis of Copper Oxide Nanoparticles from Waste Printed Circuit Boards as Photocatalyst in the Photodegradation of Tetracycline

Fariha Maryam Muhammad Faisal[1], Sheela Chandren[1,2]* and Santush Suras Kumar[1]

[1]Department of Chemistry, Faculty of Science, Universiti Teknologi Malaysia, 81310 UTM Johor Bahru, Johor, Malaysia

[2]Centre for Sustainable Nanomaterials, Ibnu Sina Institute for Scientific and Industrial Research, Universiti Teknologi Malaysia, 81310 UTM Johor Bahru, Johor, Malaysia

*Corresponding author (e-mail: sheela@utm.my)

Printed circuit boards (PCBs), can be found in any piece of electrical or electronic equipment. By recycling PCBs, copper oxide nanoparticles (CuO NPs) can be obtained, the use of which as photocatalyst has garnered a lot of attention. In this study, the recovery of CuO NPs from PCBs was presented using two approaches; hydrothermal and ammonia leaching methods. For the hydrothermal method, CuO in waste PCBs was leached out using nitric acid while the ammonia leaching method involves the leaching in ammoniacal/ammonium salt solutions. X-ray diffraction analysis showed the pure crystalline phase of CuO NPs. Field emission scanning electron microscopy images showed almost spherically-shaped NPs, with sizes ranging from 45.04 to 172.09 nm. The nitrogen sorption analysis shows the CuO NPs exhibit a type V isotherm with a pore size distribution of between 41.1 to 46.3 nm and a surface area that ranges from 3.6 to 6.8 m^2/g. The percentage of tetracycline degradation by CuO from the hydrothermal and ammonia leaching methods were 33.77% and 60.89% under UV light, respectively, and 40.61% and 64.24% under visible light, respectively, after 180 min. This study proved that CuO NPs obtained from waste PCBs showed good photocatalytic performance in the degradation of organic pollutants.

Keywords: Copper oxide (CuO); printed circuit boards (PCBs); tetracycline

Received: December 2022; Accepted: February 2023

Massive amounts of electric and electronic equipment waste have been generated in recent years due to the rapid advancement of electronic devices [1]. Electronic waste (E-waste) has been highlighted as the world's fastest-increasing waste source today, with rapid socio-economic growth and technological improvement being the key drivers. If not correctly managed, the toxic chemical components of E-waste have the potential to harm ecosystems and human health [2].

For all electronic devices, printed circuit boards (PCBs) are the most required constituents. PCB recycling is an important topic not only in terms of waste treatment but also in terms of recovering valuable resources [3]. For recovering metals from PCBs, pyrometallurgy, bio-leaching, and hydrometallurgy have all been employed extensively [4]. When compared to other processes, the hydrometallurgical route of metal recovery is more environmentally friendly since it is controlled, has a lower capital cost, and has a lower environmental effect [5].

It is also known that CuO is present in considerable amounts in PCBs. CuO occurs in the form of a mineral called tenorite, and the symmetry is monoclinic. CuO is a p-type semiconductor with a small band gap (1.2 eV) that belongs to the transition metal oxide group [6]. CuO NPs have received a lot of attention since they are highly reactive semiconductor that has a lot of potential in catalysis, making them ideal for green nanoparticle production [7].

CuO is frequently used and is one of the most important photocatalysts used in the photodegradation of organic pollutants [8]. Figure 1 shows the mechanism for the photodegradation of an organic pollutant, namely tetracycline, under UV and visible light irradiations. Tetracycline is one of the most widely used antibiotics on the planet [9]. Though tetracycline has various health advantages for people and animals, excessive usage has been linked to allergic responses in humans, bacterial resistance, and harmful to the environment. Photo-catalytic systems, such as CuO NPs, are used in AOPs, in which hydroxyl radicals are produced in the presence of electromagnetic radiation. These radicals cause pollutants to oxidize, turning them into less hazardous by-products.

†Paper presented at the Global Women Breakfast (GWB2023) Webinar

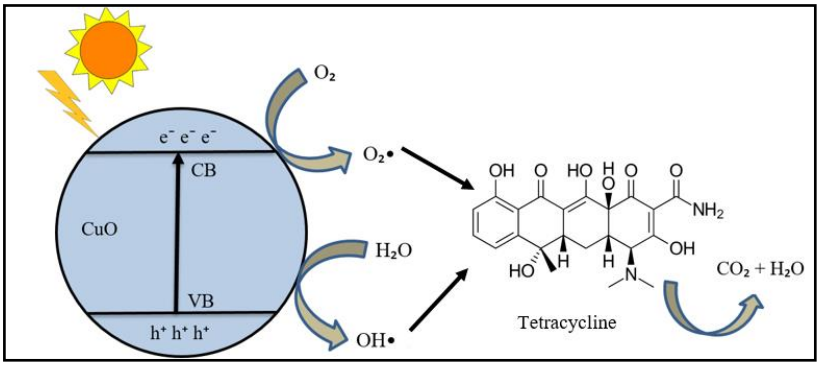

Figure 1. The mechanism for the photodegradation of tetracycline under UV and visible light irradiations.

In this study, hydrometallurgical techniques were used to extract metals progressively from PCBs, which were hydrothermal and ammonia leaching methods. Hydrothermal and ammonia leaching methods were chosen as they are more environmentally friendly when compared to other PCBs recycling technologies [5]. The physicochemical properties of the synthesized materials were determined by field emission scanning electron microscopy (FESEM) for confirmation of the morphology structure, equipped with energy-dispersive X-ray (EDX) to identify the elemental composition, X-ray diffraction (XRD) for the crystallinity studies, Fourier transform infrared (FTIR) spectroscopy for the determination of functional groups, ultraviolet-visible-near-infrared (UV-vis-NIR) spectroscopy for the optical study and the calculation of band gap energy. The synthesized materials were tested in the photodegradation of an organic pollutant, tetracycline, under UV light irradiation.

EXPERIMENTAL

Determination of PCBs Metal Composition

Chemical analysis of waste PCBs powder was performed after digestion using aqua regia (HCl: HNO_3 = 3:1) at 180 °C for 30 min. The concentration of metals present in the PCBs was analyzed by inductively coupled plasma optical emission spectroscopy (5800 ICP-OES model from Agilent Technologies) with a 40.68 MHz frequency generator.

Synthesis of CuO NPs

Hydrothermal Method

A measured quantity of solvent (4M HNO_3) was poured into the flask and heated to a pre-set temperature (70 °C) in a round bottom flask. To maintain the solid-to-liquid ratio (S/L ratio = 1/10), the required amount of the chopped PCBs was charged into the flask after the specified temperature was reached. Heating was done at the set temperature with stirring (400 rpm) and continued for 3 h. Following that, the solution was filtered using a Whatman Filter Paper Grade 1 with a diameter of 125 mm. The NPs were prepared by subjecting the leachate obtained from the hydrothermal synthesis protocol. The pH of the filtrate was made basic by adding an adequate quantity of 3M NaOH until the precipitate formed. The solution was then transferred to a Teflon-lined stainless-steel hydrothermal autoclave reactor and was put inside an oven at a pre-set temperature (140 °C) for 24 h. The particles were centrifuged and washed many times with pure water followed by pure ethanol to expel unreacted ions, then dried in a universal oven (Memmert UN-110 model) at 80 °C.

Ammonia Leaching Method

5 g of waste PCBs powder was leached using 0.5 M ammonium chloride in 8% ammonia solution with an S/L ratio of 1/10 for 1 – 4 h. The solution was then left for 24 h at room temperature. A black powder of CuO was then formed. The particles were centrifuged and washed many times with water followed by ethanol to expel unreacted ions, then dried in a universal oven (Memmert UN-110 model) at 80 °C.

Characterization

The physicochemical properties of the synthesized CuO NPs were determined by FESEM JEOL JSM-6701F model for confirmation of the morphological structure, equipped with EDX to identify the elemental composition, XRD using Bruker AXS D8 Automatic Powder Diffractometer with Cu Kα (λ=1.54060 Å) for the crystallinity studies, FTIR spectroscopy (Perkin-Elmer-1600 model series) using potassium bromide (KBr) pellets for the determination of functional groups, UV-vis-NIR spectroscopy model UV-3600plus for optical study and the calculation of band gap energy, and N_2 adsorption-desorption analysis using Micro-meritics ASAP 2020 instrument with N_2 as the adsorbed gas for determination of pore size and specific surface area.

Photodegradation of Tetracycline

The photocatalytic activities of the prepared CuO NPs were tested out in the degradation of tetracycline using a 6 W lamp from Vilber Lourmat as the UV light source. 100 mg of synthesized CuO NPs was added into the tetracycline solution (25 ppm, 100 mL) and the beaker was sealed with parafilm to avoid the evaporation of tetracycline. The tetracycline solution in the presence of the photocatalyst was placed inside the dark box and stirred using a magnetic stirrer, for 1 h to reach adsorption equilibrium. After that, the UV light was switched on and the photocatalytic reaction was performed for 3 h. 5 mL of tetracycline solution was taken out every 30 min and its concentration were determined using a UV-Vis spectrophotometer (Shimadzu UV-1800 model) at the wavelength of 200 to 800 nm. For reaction under the irradiation of visible light, Philips 18 Watt LED bulb was used instead of UV light, and the same procedures stated above were repeated.

The degradation percentage was calculated using equation 1.1 below:

$$\text{Degradation percentage } (\%) = \frac{C_0 - C}{C_0} \times 100\% \qquad 1.1$$

Where; C_0 = initial concentration of tetracycline after 1 of dark reaction

C = concentration of tetracycline after treated with UV light irradiation

RESULTS AND DISCUSSION

PCBs Metal Composition

Determination of the metal concentration of the PCBs scrap was done using ICP-OES. Table 1 below shows the result of the test. It is observed that Cu is present as the highest metal contribution, at the concentration of 83570.00 mg/kg, while Fe, Al, Pb, and Zn were found at lower levels of concentrations. The same pattern was also observed in a previous study [10].

Preparation of CuO NPs from PCBs

CuO NPs have been prepared from CuO precipitate that was extracted earlier from PCBs after the leaching process, washing, and drying of the CuO precipitate. Synthesis of CuO NPs by the hydrothermal (Figure 2 (a)) and ammonia leaching (Figure 2 (b)) methods resulted in black powders, as shown in Figure 2 below.

Table 1. The concentration of selected elements from PCB scrap.

Elements	Concentration (mg/kg)
Cu	83570.00
Fe	20.21
Al	39.64
Pb	5.26
Zn	2.11

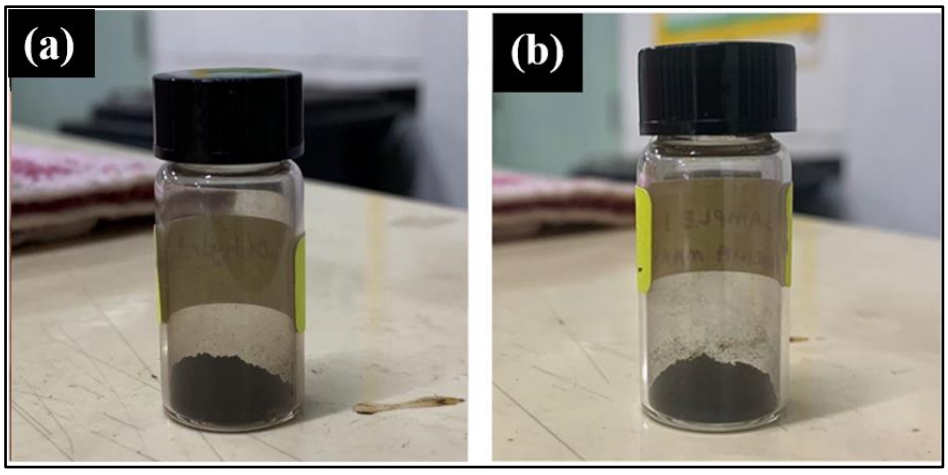

Figure 2. CuO NPs obtained from the a) hydrothermal and b) ammonia leaching methods.

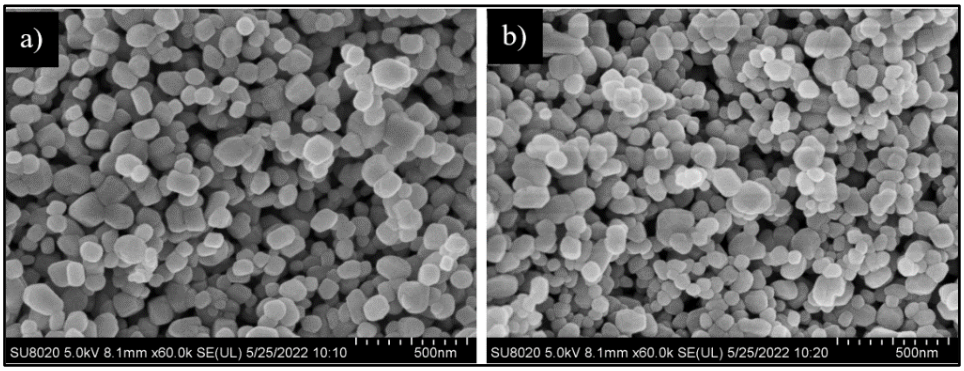

Figure 3. FESEM images of CuO NPs obtained by the a) hydrothermal method and b) ammonia leaching method at a magnification of 60000 times.

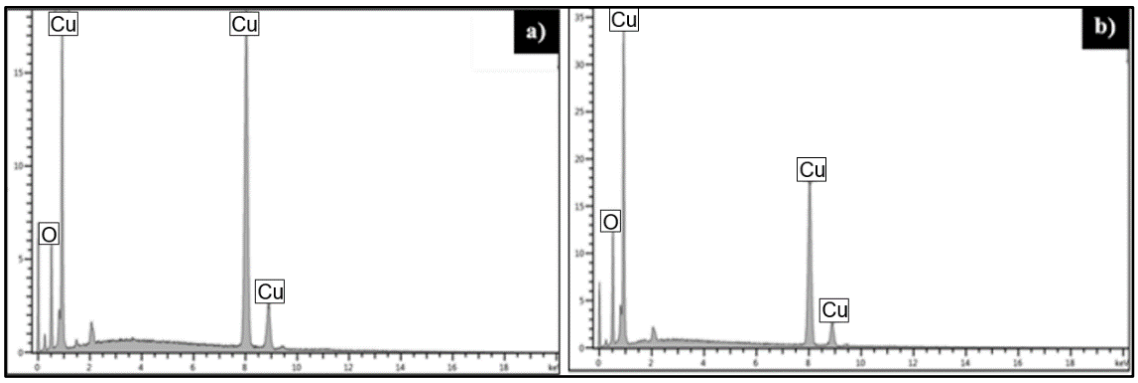

Figure 4. EDX spectra of CuO NPs obtained by the a) hydrothermal method and b) ammonia leaching method.

Physiochemical Properties of the Synthesized CuO NPs

Morphology

In Figure 3, the morphology of the CuO NPs is shown in the FESEM images with a magnification of 60000 times. The synthesized CuO NPs from both methods are almost spherical in shape with a homogenous distribution. The agglomeration of the NPs was due to the high surface tension [11]. The particle size of CuO NPs by the hydrothermal method (Figure 3 (a)) was in the range of 76.51 – 166.42 nm with an average particle size of 104.55 nm, while by the ammonia leaching method (Figure 3 (b)), the particle size was in the range of 45.04 – 172.09 nm with an average particle size of 90.52 nm. The difference in particle size is most probably due to the concentration of the leachant used during the synthesis. Furthermore, EDX analysis was performed to confirm that CuO NPs were effectively achieved. The synthesized materials primarily consist of copper (Cu), and oxygen (O), according to the analyses illustrated in Figure 4. The presence of impurities, as seen by the peak at 2.0 eV, might be due to the presence of gold (Au) used in the coating for the analysis.

Functional Groups

FTIR analysis was performed to determine the functional groups and the presence of CuO. Figure 5 shows the FTIR spectra of CuO NPs synthesized using the hydrothermal method (a) before and (b) after calcination at 450 °C for 6 h. In both spectra, peaks observed at 521.84 cm^{-1} and 517.25 cm^{-1} correspond to the Cu-O stretching bond [12]. The absorption bands at around 1381.67 cm^{-1} and 3404.70 cm^{-1} are attributed to the bending and stretching vibrations of the O-H group, respectively [13]. This is due to the absorbed water molecules on the surface of CuO NPs. Furthermore, the role of calcination was to remove organic matter present in the NPs and this can be seen from the spectrum in the calcined sample (Fig. 5 (b)), where the peak of C=C bond cannot longer be seen. However, the O-H intensity intensified after calcination, most probably due to the absorption of moisture from the surrounding. It is well known that oxide materials can absorb moisture from the ambient air [14].

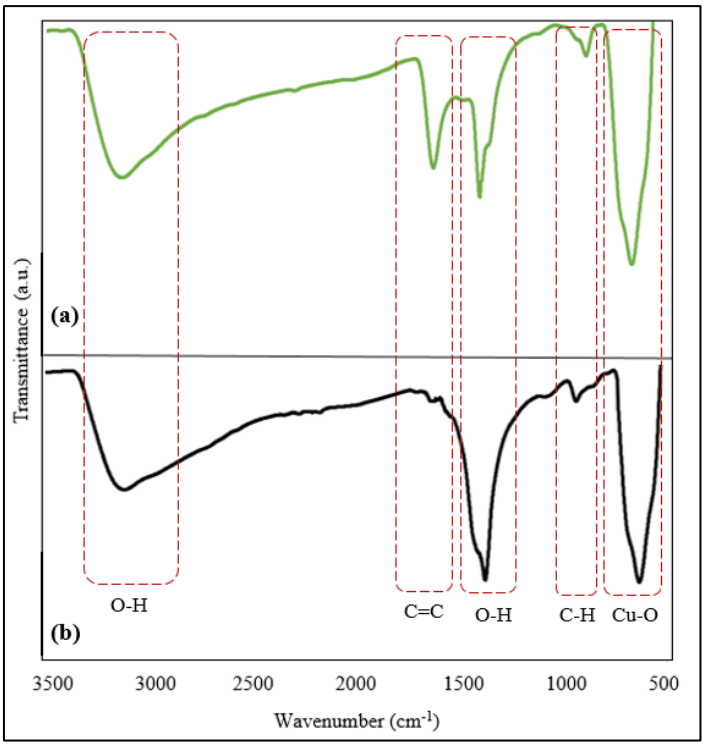

Figure 5. FTIR spectra of CuO NPs synthesized from the hydrothermal method (a) before and (b) after calcination.

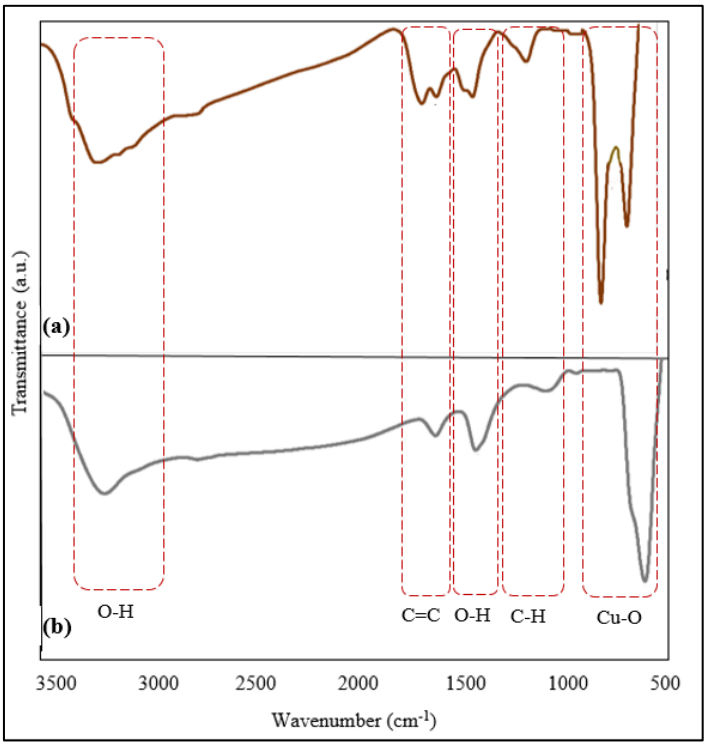

Figure 6. FTIR spectra of CuO NPs synthesized from the ammonia leaching (a) before and (b) after calcination.

Meanwhile, the FTIR spectra of the synthesized CuO NPs by the ammonia leaching method (a) before and (b) after calcination at 450 °C for 6 h are displayed in Figure 6. The study showed that there are broad absorption bands at 3418.84 cm^{-1} and 3423.78 cm^{-1}, corresponding to the O-H groups [13]. The intense absorption band at 500 – 700 cm^{-1} is attributed to the vibration of the Cu-O bond [12]. The peak in spectra

(a) at 1609.19 cm^{-1} and the reduced one in (b) at 1639.54 cm^{-1} can be assigned to the aromatic bending of the alkene group (C=C), where it was shown that calcination did not manage to completely remove the functional group. The peaks at 1300 – 1440 cm^{-1} correspond to the bending of the O-H groups due to the absorbed water molecules on the surface of CuO NPs [13]. Apart from that, the calcination of the NPs has successfully removed the C-H alkane bond that should have appeared at the region of 1328 cm^{-1}.

Crystallinity

The X-ray diffraction patterns of the synthesized CuO NPs by the hydrothermal and ammonia leaching methods are shown in Figure 7. From the figure below, the XRD pattern for CuO NPs by the hydrothermal method (Figure 7 (a)) consists of several peaks at the 2θ values of 32.44 °, 35.49 °, 38.66 °, 48.72°, 53.46 °, 58.26 °, 61.49 °, 66.19 °, 68.06 °, 72.37 ° and 75.02 °, corresponding to the (110), (002), (111), (20-2), (020), (202), (11-3), (31-1), (113), (311) and (004) planes, respectively. These peaks match the monoclinic structure of CuO, as proven by JCPDS card no: 89-5895 [15]. The diffraction peaks for CuO NPs by the ammonia leaching method (Fig. 7 (b)) can be seen at the 2θ values of 32.44 °, 35.49 °, 38.66 °, 48.72°, 53.46 °, 58.26 °, 61.49 °, 66.19 °, 68.06 °, 72.37 ° and 75.02 °, corresponding to the (110), (002), (111), (20-2), (020), (202), (11-3), (31-1), (113), (311) and (004) planes, respectively. The XRD results showed that in both methods, crystalline CuO has been successfully obtained.

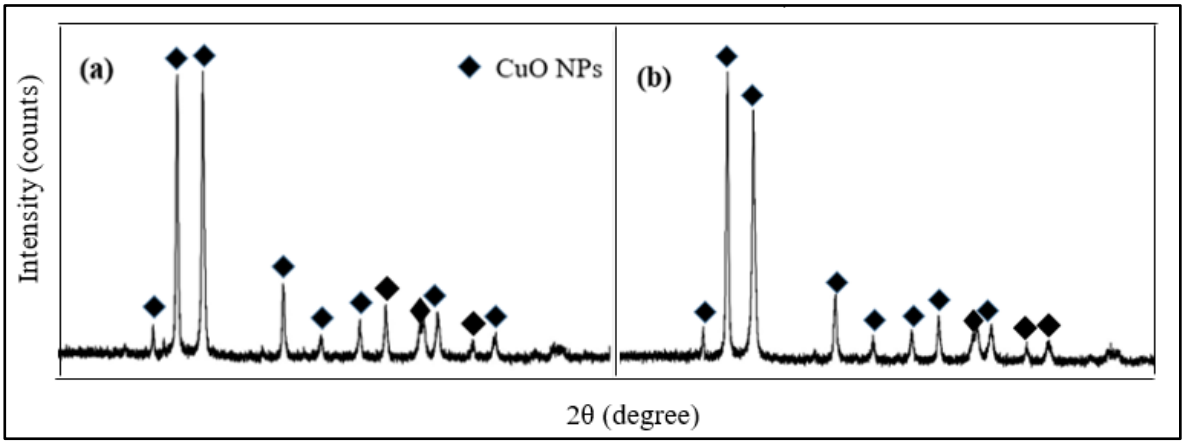

Figure 7. XRD patterns for CuO NPs obtained by (a) hydrothermal and (b) ammonia leaching methods.

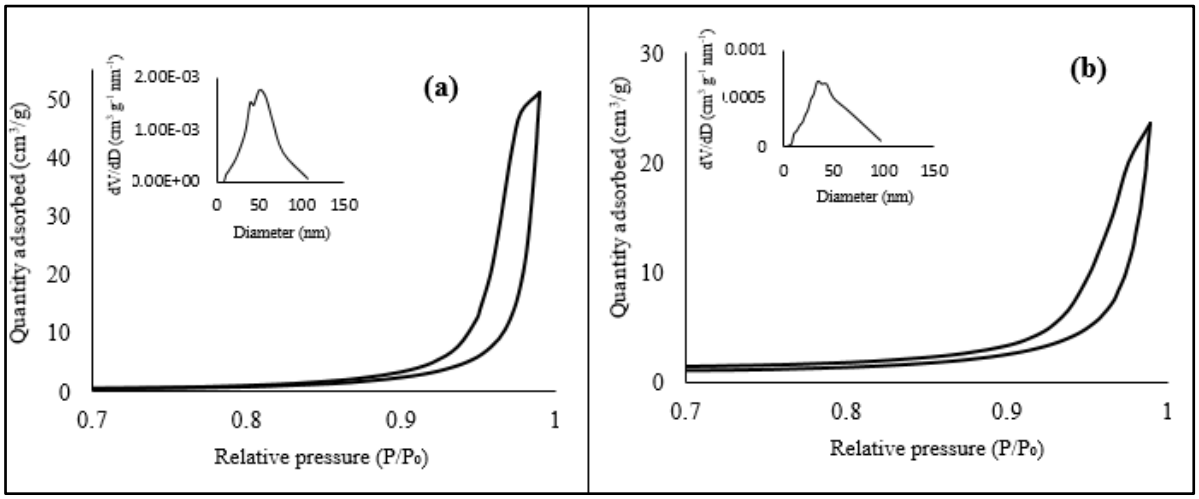

Figure 8. N_2 adsorption-desorption isotherms of CuO NPs obtained from the (a) hydrothermal method and (b) ammonia leaching method.

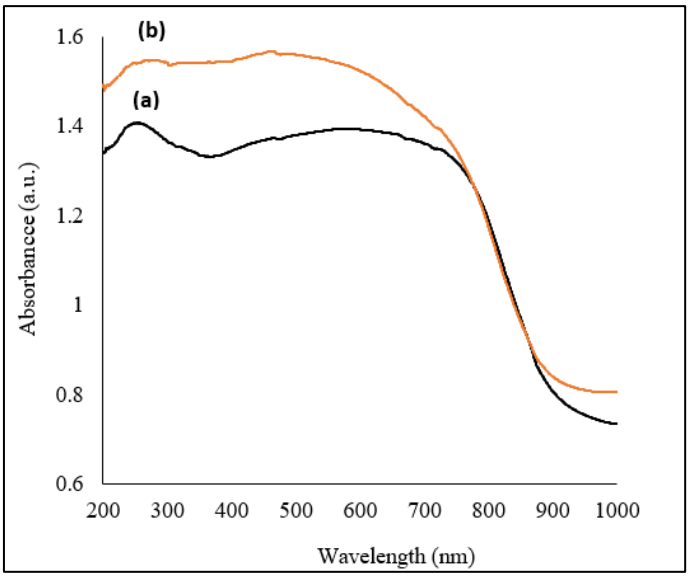

Figure 9. UV-Vis-NIR absorption spectra of CuO NPs obtained by the (a) hydrothermal method and (b) ammonia leaching method.

Porosity and Surface Area

To further obtain information about the pores of the NPs, nitrogen adsorption and desorption measurements were performed. The CuO NPs exhibit a Type V nitrogen isotherm with a hysteresis loop type H3, characteristics of mesoporous structured CuO NPs, as illustrated in Figure 8. The distribution of CuO NPs pore size was measured using the BJH method from the desorption branch and the plots are shown in the inset of Figure 8, which were 46.32 nm (Figure 8 (a)) and 41.10 nm (Figure 8 (b)) showing that the pores of both samples are in the mesopore range. The specific surface areas calculated from the BET method were 3.57 m^2/g and 6.82 m^2/g for the hydrothermal and ammonia leaching methods, respectively, while the pore volumes were 0.0366 cm^3/g and 0.0790 cm^3/g, respectively. The higher surface area for the CuO NPs obtained using the ammonia leaching method is attributable to the smaller particle sizes of the NPs produced. The higher surface area of the NPs suggests higher surface activities which are advantageous for numerous applications [16].

Optical Properties

The adsorption edge of the CuO NPs by the hydrothermal method and ammonia leaching method have estimated wavelength values of 931 nm and 935 nm, respectively, as shown in the UV-Vis-NIR absorption spectra in Figure 9. CuO NPs by the ammonia leaching method displayed a slightly higher wavelength. This is most probably caused by the smaller particle size as compared to the CuO NPs obtained by the hydrothermal method, where the absorption edge was slightly moved to a lower wavelength [17].

The band gap energy of the CuO NPs obtained was determined based on the x-intercept value from the linear extrapolation in the Tauc plot, as shown in Figure 10. The direct transitions in CuO have a broad range of values in the literature, varying between 1.6 and 3.2 eV, which is mainly due to variations in the Cu-O stoichiometry [15]. As previously reported, the band gap of 1.87 eV is found to be common for nanocrystalline CuO and considerably higher than monoclinic bulk CuO (1.2 eV), which is usually recognized as a p-type semiconductor [18]. From the Tauc plot, CuO NPs from both methods are p-type semiconductors, because they have narrow band gaps, which were 1.72 eV (Figure 10 (a)) and 1.87 eV (Figure 10 (b)).

Photocatalytic Activity of the Synthesized CuO NPs

The photocatalytic activities of CuO NPs by the hydrothermal and ammonia leaching methods were tested out in the photodegradation of tetracycline under UV and visible light irradiation. At wavelengths of 272 and 365 nm, two strong absorption peaks can be seen in Figure 11. The same observations were also obtained by Wang & Jian's work [11]. The maximum absorption wavelength for detecting the concentration of tetracycline was found to be 357 nm, which corresponds mainly to $\pi \rightarrow \pi^*$ transitions of C=C.

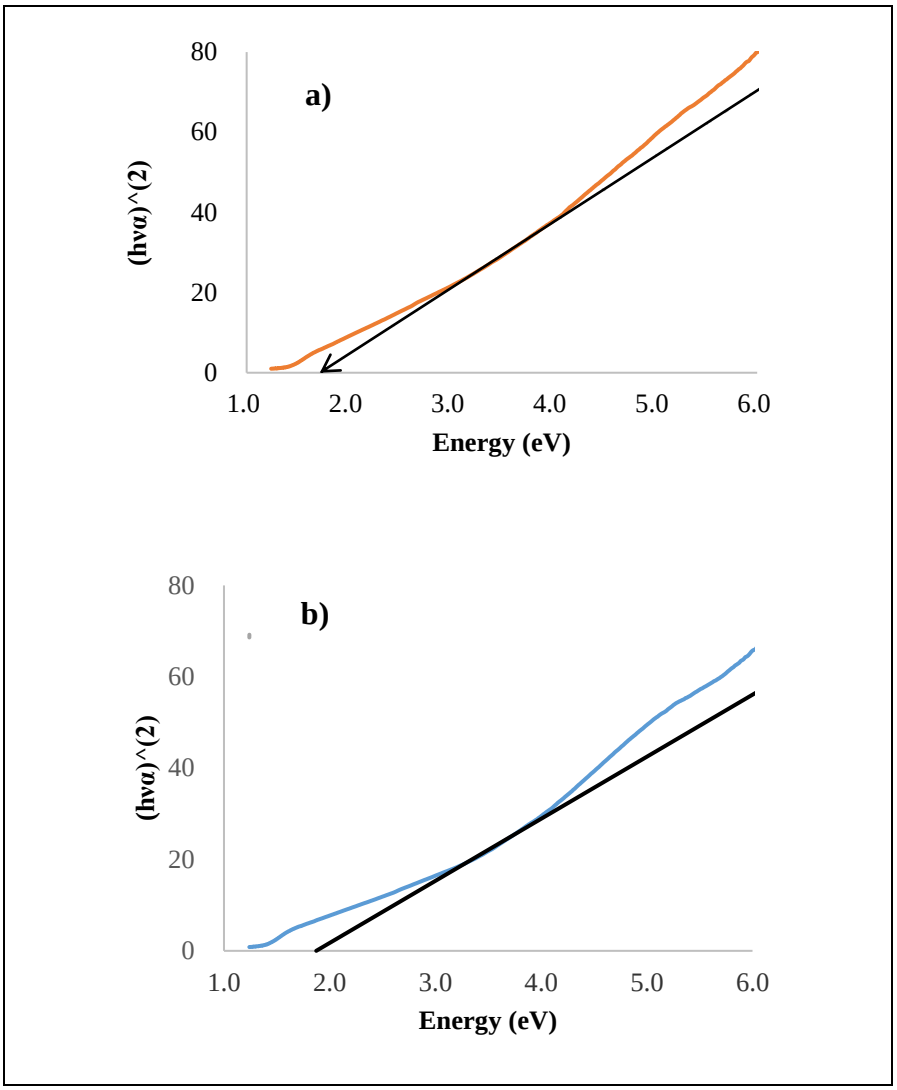

Figure 10. CuO NPs of (a) hydrothermal method and (b) ammonia leaching method.

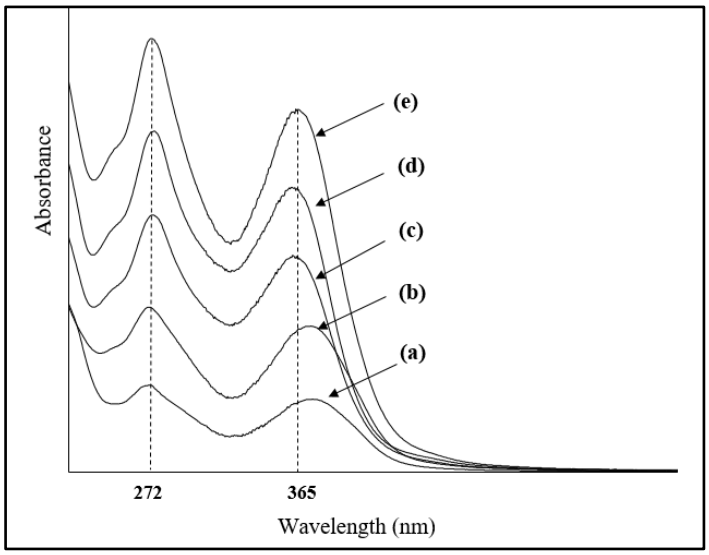

Figure 11. UV spectra of tetracycline at various concentrations (a) 5 ppm, (b) 10 ppm, (c) 15 ppm, (d) 20 ppm and (e) 25 ppm.

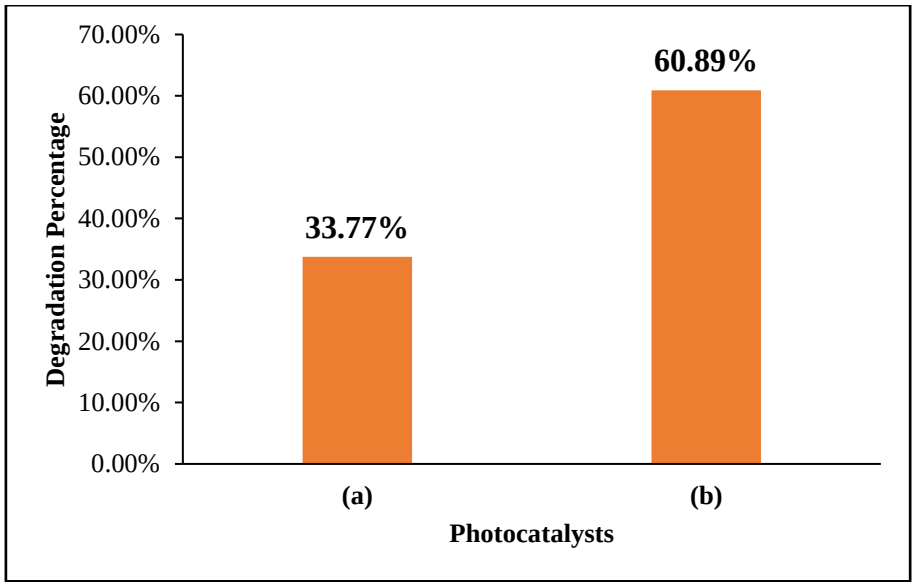

Figure 12. The degradation percentage of tetracycline under UV light irradiation by CuO NPs obtained through the (a) hydrothermal and (b) ammonia leaching methods.

Figure 12 shows the degradation percentage of tetracycline treated with CuO photocatalyst after 3 h of UV light irradiation. Comparing both the samples, CuO NPs prepared by the ammonia leaching method managed to degrade tetracycline at a higher percentage compared to CuO NPs prepared by the hydrothermal method, which was 60.89% and 33.77%, respectively.

Figure 13 shows the degradation percentage of tetracycline treated with CuO photocatalysts after 3 h of visible light irradiation. The same pattern was observed, where CuO NPs obtained through the ammonia leaching method managed to degrade tetracycline at a higher percentage compared to CuO NPs by the hydrothermal method, which was 64.24% and 40.61%, respectively.

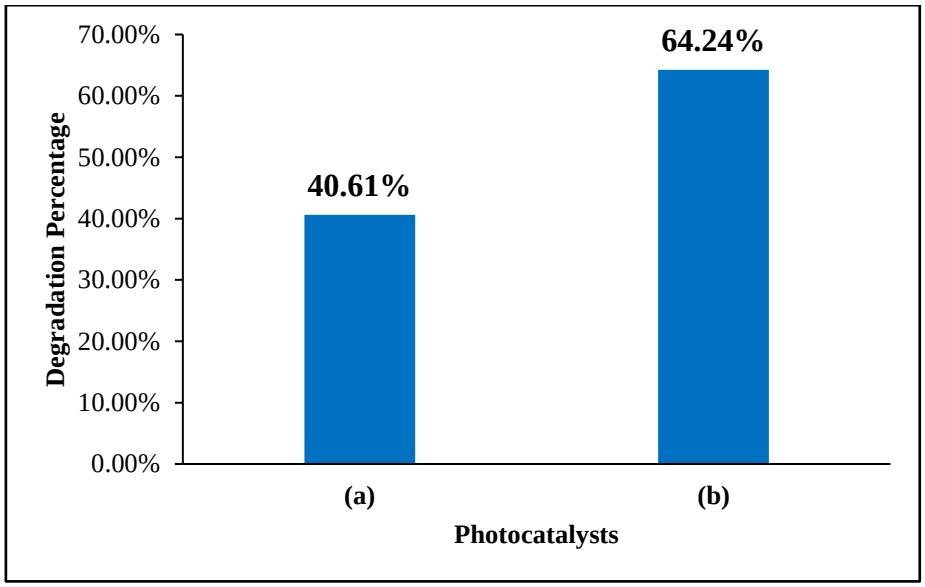

Figure 13. The degradation percentage of tetracycline under visible light irradiation by CuO NPs obtained through the (a) hydrothermal and (b) ammonia leaching methods.

Both CuO NPs by the hydrothermal and ammonia leaching methods have better visible light absorption capacities due to their band gap values, which were 1.72 eV and 1.87 eV, respectively. When exposed to visible light, they are capable of producing photogenerated electron-hole pairs. It is known that the recombination opportunities of photogenerated electron-hole pairs will be greatly reduced with the decrease of the particle size, and thus more electrons and holes will be diffused effectively to the surface to enhance the photocatalytic efficiency [19]. In the present case, it is postulated that the CuO NPs by the ammonia leaching method can promote higher efficiency of the electron-hole separation, transferring to the surface, resulting in higher photocatalytic activity due to its smaller particle size, compared to CuO NPs by the hydrothermal method.

The enhanced photocatalytic activity of CuO NPs could be attributed to several factors such as particle size, specific surface area, and the band gap energy. According to the findings of the characterization and photocatalytic activity testing, the synthesized CuO NPs using both hydrothermal and ammonia leaching methods was a successful approach. In addition, the CuO NPs prepared using the ammonia leaching method performed better in terms of photo-degradation of tetracycline when exposed to UV and visible light irradiations compared to CuO NPs obtained using the hydrothermal method. Smaller particle sizes resulted in a much greater surface area. Thus, the higher performance is most likely due to the higher surface area [19]. In conclusion, both methods can obtain CuO NPs from waste PCBs, and the ammonia leaching method showed better photocatalytic performance compared to the hydrothermal method under UV and visible light irradiations. Thus, this project was a successful approach to utilizing E-waste, which promotes the recycling of waste PCBs.

CONCLUSION

In this project, two simple and efficient methods for the preparation of CuO NPs from waste PCBs, which were the hydrothermal and ammonia leaching methods, have been carried out. From the results obtained, both methods successfully obtained spherical CuO NPs, which consist of a purely crystalline phase of CuO, with band gap energies in the CuO NPs phase range. The photodegradation results show that the synthesized CuO NPs from both methods were able to degrade the tetracycline solution under UV and visible light irradiations, where CuO NPs by the ammonia leaching method showed a higher degradation percentage of tetracycline under both UV and visible light irradiations, owing to the higher surface area. In conclusion, the CuO NPs photocatalysts generated using an environmentally friendly synthesis method showed potential as a good UV and visible light active photocatalyst, thus extraction of CuO NPs from waste PCBs will promote better E-waste management as it boosts recycling of PCBs.

ACKNOWLEDGEMENTS

The authors would like to acknowledge funding from the Ministry of Education (MOE), Malaysia, through the Fundamental Research Grant Scheme (FRGS/1/2021/STG04/UTM/02/2) and Universiti Teknologi Malaysia through the Hi-Tech (F4) Research Grant (Q.J130000.4654.00Q19).

REFERENCES

1. Akram, R., Natasha, Fahad, S., Hashmi, M. Z., Wahid (2019) Trends of electronic waste pollution and its impact on the global environment and ecosystem. *Environmental Science and Pollution Research*, **26(17)**, 16923–16938.

2. Khetriwal, D. S., Kraeuchi, P. & Widmer, R. (2009) Producer responsibility for e-waste management: Key issues for consideration - Learning from the Swiss experience. *Journal of Environmental Management*, **90(1)**, 153–165.

3. Jiang, L., Cheng, Z., Zhang, D., Song, M., Wang, Y., Luo, C., Yin, H., Li, J. & Zhang, G. (2017) The influence of e-waste recycling on the molecular ecological network of soil microbial communities in Pakistan and China. *Environmental Pollution*, **231**, 173–181.

4. Kaya, M. (2016) Recovery of metals and nonmetals from electronic waste by physical and chemical recycling processes. *Waste Management*, **57**, 64–90.

5. Weng, C. H. (2020) Water pollution prevention and state of the art treatment technologies. *Environmental Science and Pollution Research*, **27(28)**, 34583–34585.

6. Zoolfakar, A. S., Rani, R. A., Morfa, A. J., O'Mullane, A. P. & Kalantar-Zadeh, K. (2014) Nanostructured copper oxide semiconductors: A perspective on materials, synthesis methods and applications. *Journal of Materials Chemistry C*, **2(27)**, 5247–5270.

7. You, J., Guo, Y., Guo, R. & Liu, X. (2019) A review of visible light-active photocatalysts for water disinfection: Features and prospects. *Chemical Engineering Journal*, **373**, 624–641.

8. Souza, F. S., da Silva, V. V., Rosin, C. K., Hainzenreder, L., Arenzon, A. & Féris, L. A. (2018) Comparison of different advanced oxidation processes for the removal of amoxicillin in aqueous solution. *Environmental Technology (United Kingdom)*, **39(5)**, 549–557.

9. Klein, E. Y., Van Boeckel, T. P., Martinez, E.

M., Pant, S., Gandra, S., Levin, S. A., Goossens, H. & Laxminarayan, R. (2018) Global increase and geographic convergence in antibiotic consumption between 2000 and 2015. *Proceedings of the National Academy of Sciences of the United States of America*, **115(15)**, 3463–3470.

10. Adie, G. U., Balogun, O. E., Li, J. H. & Osibanjo, O. (2014) Trends in toxic metal levels in discarded laptop printed circuit boards. *Advanced Materials Research*, **878**, 413–419.

11. Mello, V. S., Faria, E. A., Alves, S. M. & Scandian, C. (2020) Enhancing CuO nanolubricant performance using dispersing agents. *Tribology International*, **150**, 106338.

12. Sodeifian, G. & Behnood, R. (2020) Hydrothermal Synthesis of N-Doped GQD/CuO and N-Doped GQD/ZnO Nanophotocatalysts for MB Dye Removal Under Visible Light Irradiation: Evaluation of a New Procedure to Produce N-Doped GQD/ZnO. *Journal of Inorganic and Organometallic Polymers and Materials*, **30(4)**, 1266–1280.

13. Phiwdang, K., Suphankij, S., Mekprasart, W. & Pecharapa, W. (2013) Synthesis of CuO nano-particles by precipitation method using different precursors. *Energy Procedia*, **34**, 740–745.

14. Shi, W., Song, S. & Zhang, H. (2013) Hydro-thermal synthetic strategies of inorganic semi-conducting nanostructures. *Chemical Society Reviews*, **42(13)**, 5714–5743.

15. Sundar, S., Venkatachalam, G. & Kwon, S. J. (2018) Biosynthesis of copper oxide (CuO) nanowires and their use for the electrochemical sensing of dopamine. *Nanomaterials*, **8(10)**, 823

16. Wang, C. & Jian, J. -J. (2015) Degradation and Detoxicity of Tetracycline by an Enhanced Sonolysis. *Journal of Water and Environment Technology*, **13(4)**, 325–334.

17. Saion, E., Gharibshahi, E. & Naghavi, K. (2013) Size-controlled and optical properties of mono-dispersed silver nanoparticles synthesized by the radiolytic reduction method. *International Journal of Molecular Sciences*, **14(4)**, 7880–7896.

18. Hu, C., Li, P., Zhang, W., Che, Y., Sun, Y., Chi, F. & Lv, Y. (2017) Effect of cupric salts ($Cu(NO_3)_2$, $CuSO_4$, $Cu(CH_3COO)_2$) on $Cu_2(OH)PO_4$ morphology for photocatalytic degradation of 2,4-dichlorophenol under near-infrared light irradiation. *Materials Research*, **20**, 407–412.

19. Shankaraiah, G., Saritha, P., Bhagawan, D., Himabindu, V. & Vidyavathi, S. (2017) Photo-chemical oxidation of antibiotic gemifloxacin in aqueous solutions – A comparative study. *South African Journal of Chemical Engineering*, **24**, 8–16.